Ion Beam Extraction and Electron Emission from the Miniature Microwave Discharge Ion Engine μ1

IEPC-2009-178

Presented at the 31st International Electric Propulsion Conference,
University of Michigan • Ann Arbor, Michigan • USA
September 20 – 24, 2009

Hiroyuki Koizumi[1] and Hitoshi Kuninaka[2]
Institute of Space and Astronautical Science of the Japan Aerospace Exploration Agency
Sagamihara, Kanagawa, 229-8510, Japan

Abstract: In this study, we are proposing a new ion engine system to switch the operation of ion engine mode and neutralizer mode. This system eliminates a device dedicated for neutralizer and contributes the weight reduction of microspacecraft. However, completely different natures of ion and electron make it difficult to develop a plasma source suitable for both ion beam extraction and electron emission. Herein we have developed a special grid system dedicated for this switching operation. This grid system has two different types of apertures for ions and electrons respectively. The experiment showed it had sufficient performances of ion beam current for thrust and electron emission for the neutralization. The plasma source consumes 1.0 W microwave power and 0.15 sccm mass flow rate under the typical condition. The thruster can provide 3.3 mA ion beam in ion engine mode and neutralize the same amount of ion beam by the contact voltage below 40 V in neutralizer mode.

I. Introduction

IN recent years, research and development of small spacecraft have extensively grown up in the world and a number of small spacecraft have been successfully launched and operated.[1-8)] Moreover, an increasing number of planned small spacecraft missions are in need of propulsive capability. Propulsion devices supply the spacecraft with attitude control, station keeping, and orbit transfer. Furthermore, it enables future spacecraft missions such as drag free control from atmospheric or solar pressure, precise constellation flight for interferometer missions, and deorbiting maneuver of end-of-life spacecraft into the atmosphere. The arrival of propulsion devices suitable for small spacecraft, namely micro-propulsion, is awaited.[9)]

Ion engines[10)] are promising propulsion devices not only for standard-sized spacecraft but also for small spacecraft. Their characteristics of high specific impulse (3000 s), high thrust efficiency (50 %), usage of inert propellant (xenon), and continuously controllable thrust meet the requirements for small spacecraft missions. Several studies on miniature ion engines have been conducted to date for several different types of the plasma generators, namely direct current electron discharges,[11,12)] radio frequency discharges,[13)] and microwave discharges.[14-17)]

In spite of these benefits, however, miniature ion engines have not been employed on small spacecraft yet. This is mainly caused by two reasons. One reason is severe limitation of the electrical power available on small spacecraft. In general, electrical power generated in small spacecraft is about 1 W/kg. Therefore, for example, available power in 10 – 50 kg small spacecraft was estimated at only 10 – 50 W. The miniature ion engines developed to date require total power in the range of 30 W at least. The other reason is difficulty of developing a

[1] Assistant Professor, Department of Space Transportation Engineering, koizumi.hiroyuki@jaxa.jp
[2] Professor, Department of Space Transportation Engineering, kuninaka@isas.jaxa.jp

miniature neutralizer suitable for a miniature ion engine. A neutralizer emits electrons for the neutralization of ion beam and it has no contribution to the thrust. Hence it is usually designed and developed to be much smaller than the thruster itself. However, it would be very difficult to develop a ultra small and low power neutralizer for a miniature ion engine.

In order to solve the first problem, we developed a miniature ECR discharge ion engine driven by 1.0 W microwave power and 6.0 W ion acceleration power.[18] This miniature ion engine is named as μ1 ("mu-one"), due to the 1-cm-class beam diameter and 1-W-class microwave power. It is the smallest ion engine in the "μ" series of ion engines developed in ISAS of JAXA.19-21) The μ1 has the 250 W/A ion production cost and 37 % mass utilization efficiency for 1.0 W microwave input power and 0.15 sccm xenon mass flow.

For the second problem, we have proposed a novel ion engine system switching the operation of ion beam source and electron emission source.[22,23] This system is to install multiple plasma sources and each plasma source is used as either an ion beam source or a neutralizing electron source. The operational mode is selected by electrical connections. We are referring this operation as "switching operation" and its conceptual illustration is shown in Fig. 1. This switching operation is to use an ion thruster which is not operated as a neutralizer for another ion thruster. There is not in need of device dedicated for a neutralizer and it enables the weight reduction of the system. In addition, we are proposing to set these plasma sources in a distributed pattern on the spacecraft. The combination of multiple plasma sources enables spacecraft translation as well as attitude control with respect to multiple axes. It is important to unite several devices with suitable functions into one multi-function-device for the miniaturization of spacecraft. In the past study, we demonstrated that the above concept can be realized by using miniature ion engines.[22,23] In that study, however, only the concept was verified using the prototype model of the μ1 with poor performance. It consumes 5.0 W microwave power and 0.5 sccm xenon flow rate, and provided 4 – 5 mA ion beam current. This performance is too poor to be applied to actual spacecraft.

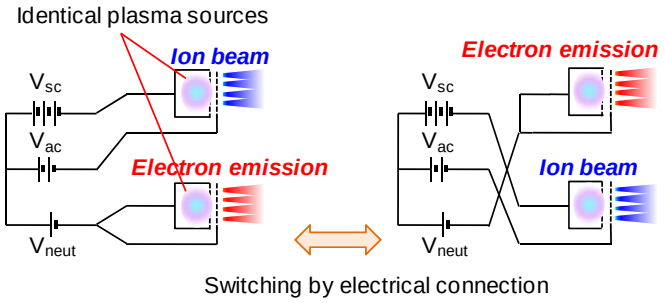

Fig. 1 Conceptual diagram to switch ion beam operation and neutralizer operation of a pair of plasma sources.

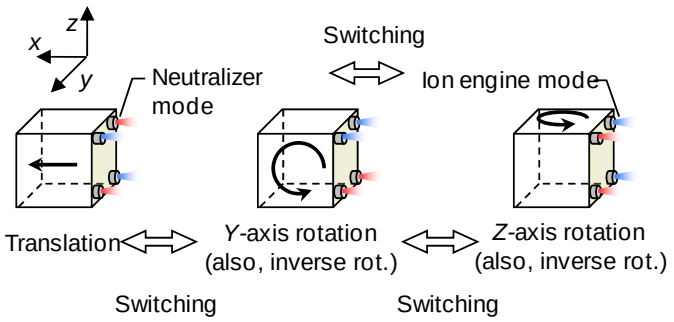

Fig. 2 Distributed ion thrusters on spacecraft to give the craft a lot of types of motions.

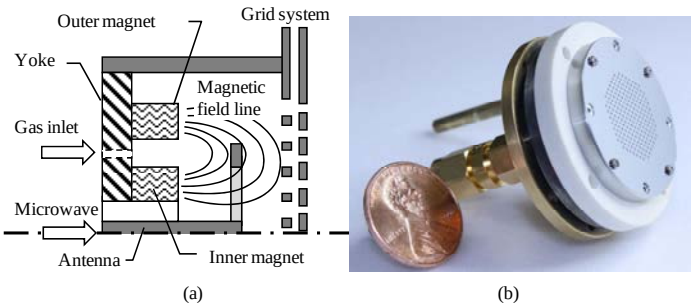

Fig. 3 Schematic illustration and picture of the miniature ion engine μ1.

The objective of this study is to realize the switching operation with high performance enough to be applied to microspacecraft. The major challenge is to optimize the plasma source for both ion beam extraction and electron emission. The above-mentioned ion engine μ1 was optimized only for ion beam extraction and not for electron emission. It is necessary to find out a configuration suitable for both operation modes. However completely different natures of ion and electron makes it difficult.

In this study, we have developed a special grid system dedicated for the switching operation and demonstrated the switching operation. This paper consists of three different experiments. First, the typical operation of the μ1 ion engine will be shown. Secondly, we have measured the fundamental characteristics of electron emission from the miniature ion engine μ1. A new grid system designed based

on the result of electron emission characteristics will be introduced. Finally, we will show the successful demonstration of the switching operation and their performance.

II. Experimental setup and method

In this study, we have performed three different experiments: ion engine operation of μ1, electron emission experiment, and switching operation.

A. Operation of the ion engine μ1

The μ1 ion engine has a discharge chamber of cylindrical shape with 20 mm diameter. The schematic illustration and the picture of the μ1 ion engine are shown in Fig. 1. Two ring-shaped permanent magnets are installed on the bottom of the chamber. The magnets form a maximum magnetic field of 0.30 T on the magnet surface and minimum field of 0.05 T at the furthest point from the magnet. The resulting magnetic field also represents a magnetic bottle which inhibits electron loss. A two-grid ion accelerator system was placed across the downstream end of the discharge chamber. The grids are made of molybdenum by chemically etching 211 apertures within a 16 mm diameter region. The configuration of these grids was designed by Nakayama et al. for a miniature ion engine, MINIT16. Detailed grid geometries are shown in Table 1. This grid system is referred herein as "nominal grid" to distinguish it from the after-mentioned "switching grid". Voltages of screen and accelerator grids were set at 1500V and -350 V respectively. The electrical connections are shown in Fig. 1 (a).

Microwave power of 4.20 GHz was introduced into the chamber using a ring-shaped antenna extending from an inner conductive part of the microwave transmission cable. The antenna configuration was matched to the plasma impedance. The microwave power line was isolated from the ground potential by a DC-block. Both, the discharge chamber and DC block were set to high positive voltage and were covered by a plasma screen.

Working gas (xenon) was fed through holes in the yoke plate and between the two magnets. A gas isolator was installed between the thruster and the gas feeding system. Mass flow rate was controlled using a mass flow controller for xenon with a maximum flow rate of 1.0 sccm (98 μg/s for xenon) and accuracy of ±1% with respect to the maximum flow rate.

Table. 1 Grid geometries of the nominal grid and switching grid.

Grid		Thickness, mm	Diameter, mm	Gap, mm	Number of holes
Nominal grid	Screen	0.20	0.72	0.25	211
	Accel.	0.30	0.40		
Switching grid	Screen A	0.20	0.72	0.25	169
	Screen B		2.20		6
	Accel. A	0.40	0.40		169
	Accel. B		1.80		6

B. Electron emission experiment

Fundamental characteristics of electron emission from the μ1 discharge chamber were investigated by using aluminum orifice plates with a single aperture. These plates are referred to herein

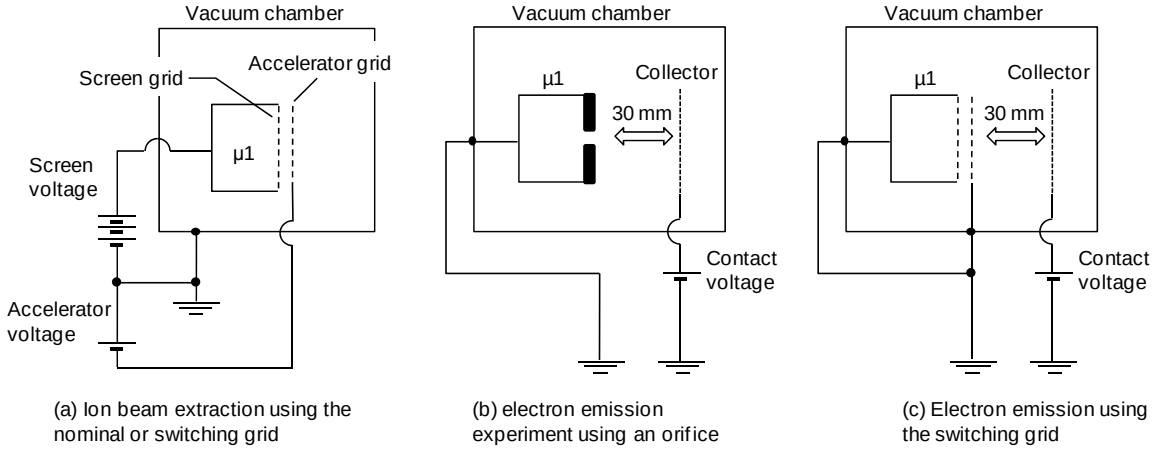

(a) Ion beam extraction using the nominal or switching grid

(b) electron emission experiment using an orifice

(c) Electron emission using the switching grid

Fig. 4 Electrical connections of (a) ion engine mode operations, (b) electron emission experiment, and (c) electron emission using the switching grid.

as electron emission orifices. The orifice was installed to the µ1 instead of the grid system. Electrons were extracted through the apertures by applying positive voltage to a collector plate placed in front of the µ1. Electrical connections for this experiment is shown in

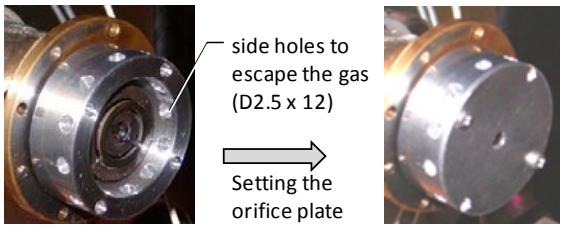

Fig. 5 Picture of the electron emission experiment.

Electron current to the collector was measured for many configurations of the aperture. The diameter was changed from 1.0 to 4.0 mm and its position was changed from 0.0 to 8.0 mm in radial direction. Totally twelve pieces of orifice plates were prepared. Fig. 3 shows the µ1 with installing one of the electron emission orifices. All of the electron emission orifices have much lower gas conductance than the nominal grid system. In this electron emission experiment, twelve holes were opened in the side wall in order to match the gas conductance.

C. Switching operation of the ion engine µ1

Based on the result of the above-mentioned electron emission experiment, a special ion accelerator grid was designed. As shown in the later section, the electron current experiment concluded that there was a minimum limit of the diameter for the electron emission. On the other hand, ion beam extraction requires a small diameter to maintain good confinement of neutral gas. Then these two requirements conflict each other. In order to solve this problem, we have developed a special grid system with two different size apertures, which is referred herein as to "switching grid". The conceptual diagram and the picture of the switching grid are shown in Fig. 4 and the specification is shown in Table. 1.

In this study, two µ1 thrusters using the switching grid were prepared. Both thrusters have the same setting and we refer them herein as µ1-A and µ1-B respectively. We performed two kinds of experiments using these µ1 thrusters. One is the experiment of ion beam extraction and electron emission from the single thruster. This was performed to identify the performance of each thruster. The other experiment is the simultaneous operation of the two thrusters, where one is operated in ion engine mode and the other is operated in neutralizer mode. In this experiment, contact voltage of the neutralizer mode thruster was adjusted to accomplish the ion beam neutralization. The base (common) potential of the ion thruster system (or spacecraft) was isolated from the ground potential and connected to it through a current measurement resistance (1.00 kΩ). We assumed that neutralization was

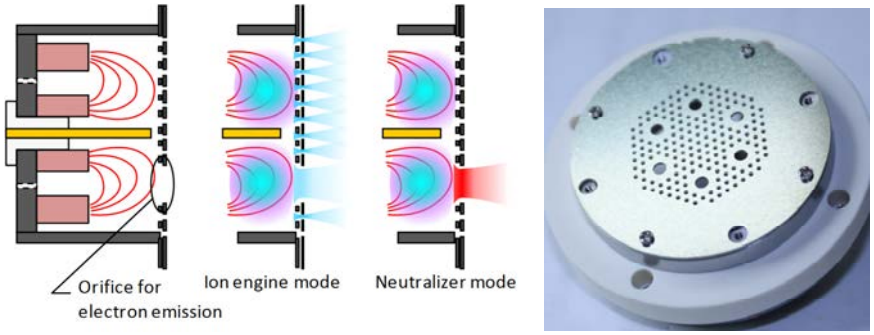

Fig. 6 Conceptual diagram and picture of the switching grid.

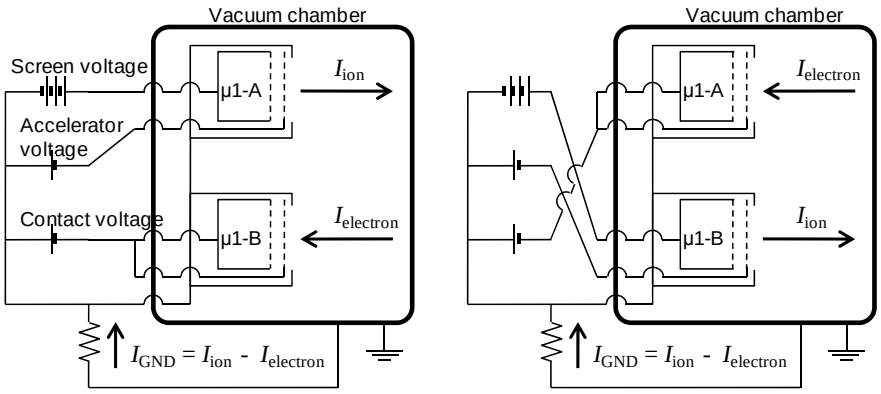

(a) µ1-A: ion engine mode
µ1-B: neutralizer mode

(b) µ1-A: neutralizer mode,
µ1-B: ion engine mode

Fig. 7 Electrical connections of the switching operation

accomplished when the current which came back from the ground (I_{GND}) became zero by adjusting the contact voltage. Contact voltages which satisfy the neutralization were measured with several microwave powers and mass flow rates. Ion engine mode and neutralizer mode were switched each other, which is referred as to the switching operation, and both characteristics were obtained. In the ion engine mode, the voltages of screen and accelerator grids were set at 1500V and -500 V respectively. The low accelerator voltage was to prevent the electron back streaming due to the larger beam apertures of the switching grid.

D. Measurement method

For the experiments of the above sections A and B, ion beam current or electron emission current was measured for the input microwave power and mass flow rate. Input microwave power was continuously swept between 0 and 5 W. First, microwave power was set around 0.1 W, gradually increased up to 5.0 W, and again decreased down to 0 W. The period of this round-trip sweeping took 20 – 40 s. During a sweeping, ion beam current or electron emission current was recorded with 200 Hz sampling rate. The ion beam current was calculated by subtracting the accelerator current from the screen current. The electron emission current is the current entering into the collector plate. The swept power range was divided into a hundred intervals, and obtained data of 4,000 – 8,000 points were averaged over each interval. During the above power sweeping, mass flow rate was fixed.

For the experiment of the section C, ion beam current and contact voltage were measured for the microwave power and mass flow rate. The contact voltage was adjusted to realize the neutralization of ion beam, whenever the microwave power or mass flow rate was changed. The two ion thrusters were set under the same microwave power and mass flow rate.

In this study, input and reflected microwave powers are referred to as forward and backward powers right behind the thruster head. Both powers were measured at the microwave power source. The measured values are then corrected by the calibrated transmission losses between the power source and the thruster head. The uncertainties of the input and the reflected power are within ±5 % error.

All the experiments were carried out in a 1.0 m diameter, 1.4 m long vacuum chamber. The chamber is evacuated by a rotary pump of 1300 L/min and a turbo molecular pump of 800 L/s for N2. The operating pressures during the experiment were between $4 – 8 \times 10^{-3}$ Pa at 50 μg/s xenon flow. The chamber is made of stainless steel and is used as the ground reference for all tests.

III. Experimental Results

A. Performance of the ion engine operation

Ion beam extraction of 4.0 mA was achieved at input microwave power of 1.0 W, which corresponds to 250 W/A ion production cost. This performance satisfied our initial target. The dependence of the ion beam on the input power is shown in Fig. 8 (a). Ion beam current increased with input microwave power at all of the mass flow rate that were studied. In the high power region of more than 1.0 W, the beam current started to be saturated. This

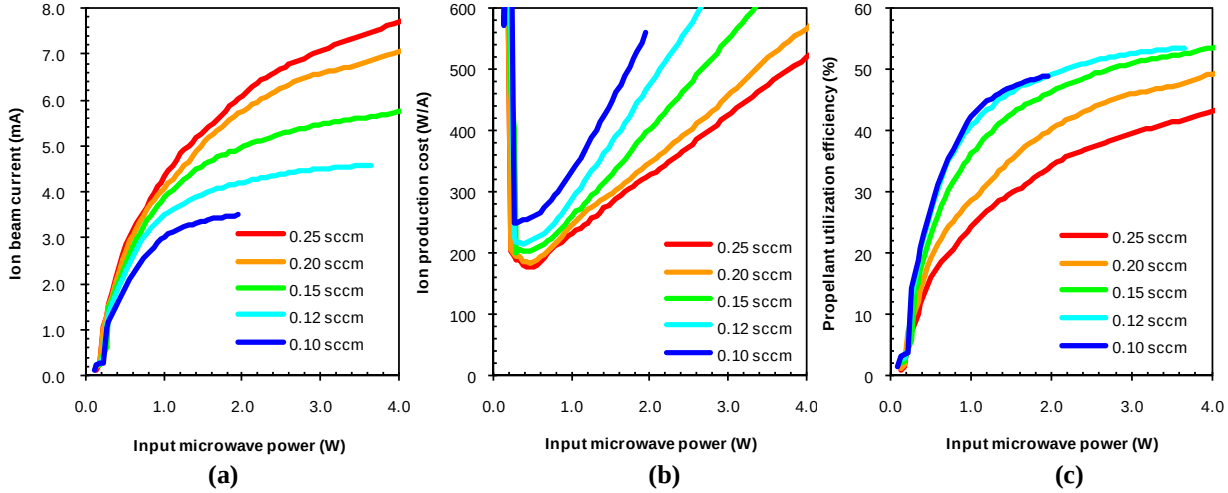

Fig. 8 Performance of the ion engine μ1 using the nominal grid: (a) ion beam current, (b) ion production cost, and (c) propellant utilization efficiency.

saturation trend was more significant at lower mass flow rates. The ion beam could be extracted even in extremely low power range of 0.2 – 1.0 W. Below the power 0.2 W, the plasma was extinguished and no more beam current was measured. Minimal differences in beam current versus microwave input power traces were observed at flow rates greater than 0.20 sccm. At lower flow rates, the differences were much more pronounced. At 1.0 W microwave power operation, beam current was varied as 3.3 – 4.2 mA depending on the mass flow rate of 0.10 – 0.25 sccm. Ion production cost dependence was shown in Fig. 8 (b). The minimum ion cost is less than 200 W/A with input microwave power of 0.5 W and mass flow rate of over 0.20 sccm. The ion cost at 1.0 W microwave ranged from 230 – 290 W/A with the mass flow rate of 0.25 – 0.12 sccm. This discharge loss is as low as standard ion engines and the lowest ever in all developed miniature ion engines. In contrast to the good discharge loss, propellant utilization efficiency was less than 55 % for all the rages, which is shown in Fig. 8 (c). This was not too low considering the small size of the μ1. Effective plasma production is achieved by decreasing the fraction of the electrons that are directly lost to the wall without making an ionization collision. Generally, electron confinement time is determined by the geometry of the system and it becomes shorter by scaling down. On the other hand, electron mean free time for ionization collision is determined by the neutral gas density. Therefore the effective plasma production in small size system requires higher neutral density and it leads to high the mass flow rate and reduction of the propellant utilization efficiency.

B. Electron emission experiment

In the experiment of electron emission using single-aperture orifices, it was found that electron emission current was largely affected by both input microwave power and orifice configuration. On the other hand, mass flow rate gave little effect on the current. The hysteresis of power during going up or down was negligible. Fig. 9 summarizes the effect of the diameter and position of the aperture. The emission current was averaged between 0.5 and 1.5 W input microwave powers, and they are plotted for the aperture diameter and radial position. The power of 0.5 to 1.5 W is the target power range of the μ1 system.

As a result, we got two important conclusions: 1) there was a minimum threshold for diameter and 2) the best position was above the ring-antenna. The first result, existence of a minimum threshold for diameter, led us to design the switching grid that has two different diameter apertures, as shown in the previous chapter. The design of the switching grid had several options for larger apertures of electron emission. For example, single aperture of 3.0 mm diameter would result in the same current of double apertures of 2.0 mm diameter based on the result of Fig. 9 (a). In this point, we selected “a lot of small apertures” to decrease electron backstreaming and designed six apertures of 1.8 mm diameter. However, concern about the electron back streaming still remained and we conducted the experiment measuring it, which will be described in the later section.

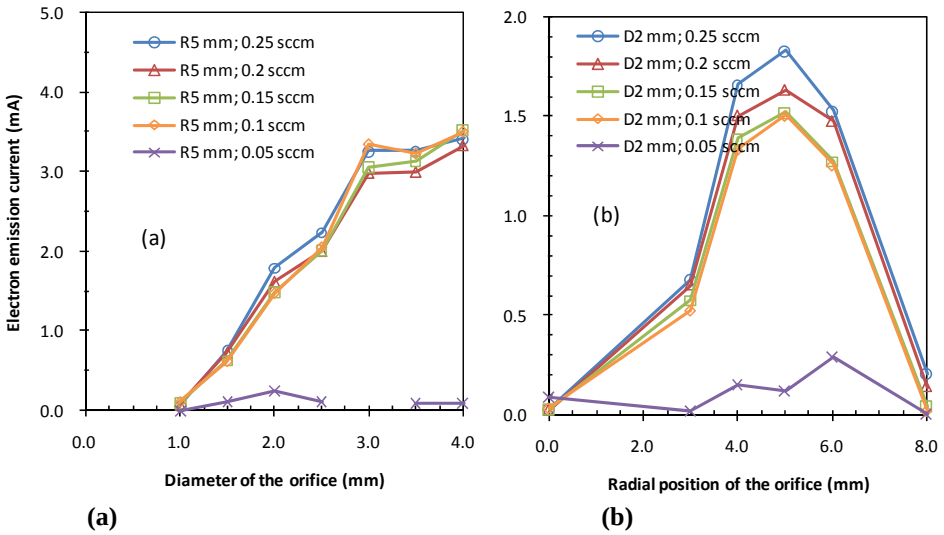

(a) **(b)**

Fig. 9 Electron emission current from the single aperture orifices; (a) dependence on the aperture diameter and (b) dependence on the position of it.

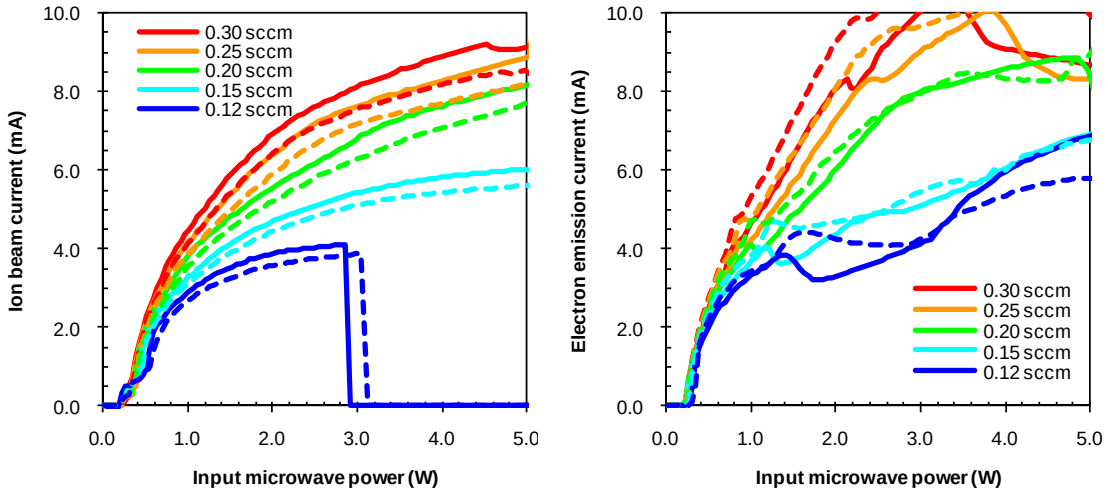

(a) **(b)**

Fig. 10 Current dependence of two thrusters with the same setting; (a) ion beam current and (b) electron emission current. Solid line is the μ1-A and dashed line is the μ1-B

C. Switching operation; single operation

The switching grid resulted in successful operation for the ion beam extraction and electron emission. Fig. 10 shows the characteristics of ion beam current (Fig. 10 (a)) and electron current (Fig. 10 (b)) for two μ1 thrusters: μ1-A and μ1-B. These data were obtained under single operation of each thruster using the electrical connection shown in Fig. 4(a) and Fig. 4(c). For each thruster experiment, ion beam and electron currents were measured sequentially by switching the outside electrical connections without opening the vacuum chamber. In this figure, solid line shows the result of the μ1-A and dashed line shows the result of μ1-B. Whereas we designed both thrusters in the equivalent setting, the obtained ion beam and electron currents showed slightly different result. Although we have not found the cause of this difference, it would not become crucial problem for the switching operation using these two μ1 thrusters.

The dependence of the ion beam on the power and flow rate was similar with the nominal operation of μ1. However, the absolute value of the current was slightly lower for the same mass flow rate. It would be caused by the reduction of the neutral particle confinement. The switching gird has the total area of the accelerator grid apertures higher than the nominal grid by 38%.

Electron currents were sufficient to neutralize the ion beam current with the operational conditions, as shown in Fig. 10 (b). In other word, the electron currents were higher than ion beam current for all the microwave power and mass flow rate. In this experiment, the contact voltage was set to fixed value of 80 V and the target plate was set at 30 mm away from the thruster.

Electron backstreaming was the great concern for the switching grid due to its large apertures. The screen current was measured for several accelerator voltages to confirm the electron backstreaming. The screen voltage was adjusted to fix the voltage gap between screen and accelerator grids. The three different voltage gaps were examined: 1500, 1800, and 2000 V. In this experiment, a hot filament was installed in front of the μ1 ion thruster to provide enough electrons in background. Actually, the hot filament emitted the electron more than 20 mA. The result is shown in Fig. 11. Screen

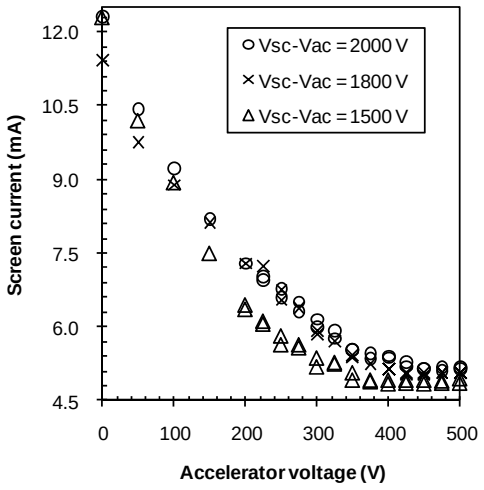

Fig. 11 Backstreaming electron for the switching grid operation.

current is greatly increased when accelerator voltage is decreased down to zero. This is clearly caused by the electron backstreaming. When the accelerator voltage is increased, the curve of the screen current became flat and converged. This means that there is no electron backstreaming and the threshold would be 400 – 450 V for gap voltages of 1500 – 2000 V.

D. Switching operation; coupling operation of two thrusters

The ion beam exhausted by a μ1 thruster was successfully neutralized by electron emission from another μ1 thruster. Two μ1 thrusters (μ1-A and μ1-B) were installed with the distance of 72 mm between the centers. Both thrusters were operated in the same conditions for microwave power and mass flow rate and one is set as ion engine mode and the other is set as neutralizer mode. The electrical connection is shown in Fig. 7. The contact voltage of the neutralizer mode thruster was adjusted to achieve the neutralization. Both modes are switched by outside electrical connection. Fig. 12 shows the pictures of these operations. The operational pictures were taken with the exposure time of 2.0 s, F-number of 5.6, and ISO sensitivity of 1600. In these pictures, plumes of the ion engine mode can be clearly recognized. Also, several beam lets which correspond to large apertures can be found. Neutralizer mode thruster emits weak and vague light near the grid.

The contact voltage that achieves the ion beam neutralization was measured with several microwave powers (0.5 to 4.0 W by 0.5 W step) and mass flow rates. The result is shown in Fig. 13. In Fig. 13 (a), μ1-A was operated as ion engine mode and μ1-B was operated as neutralizer mode and in Fig. 13 (b) the modes were switched. The characteristics of the contact voltage is different between Fig. 13(a) and Fig. 13(b). It would be due to the difference of each thruster performance shown in Fig. 10. This dependence must be identical if the two thrusters have the same performance. In this configuration, we have found that beam neutralization requires the contact voltage of below 85 V for all the tested condition. For microwave power lower than 1.5 W, the contact voltage are less than 50 V. These values are much lower than the ion production cost and would be reasonable for the application to the spacecraft.

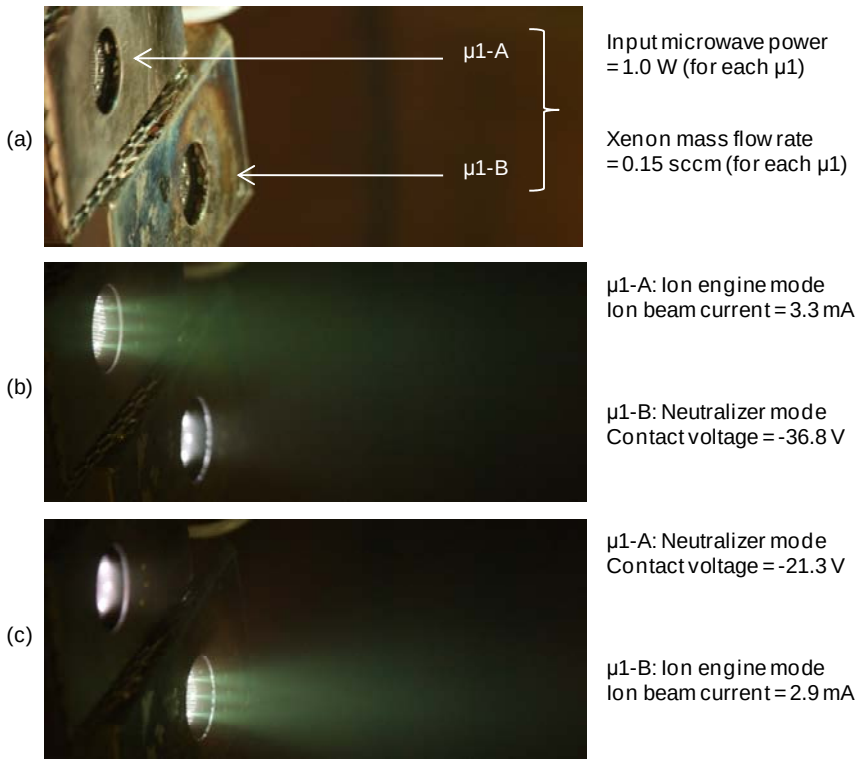

Fig. 12 Switching operation of ion engine mode and neutralizer mode using two μ1 thrusters: μ1-A and μ1-B.

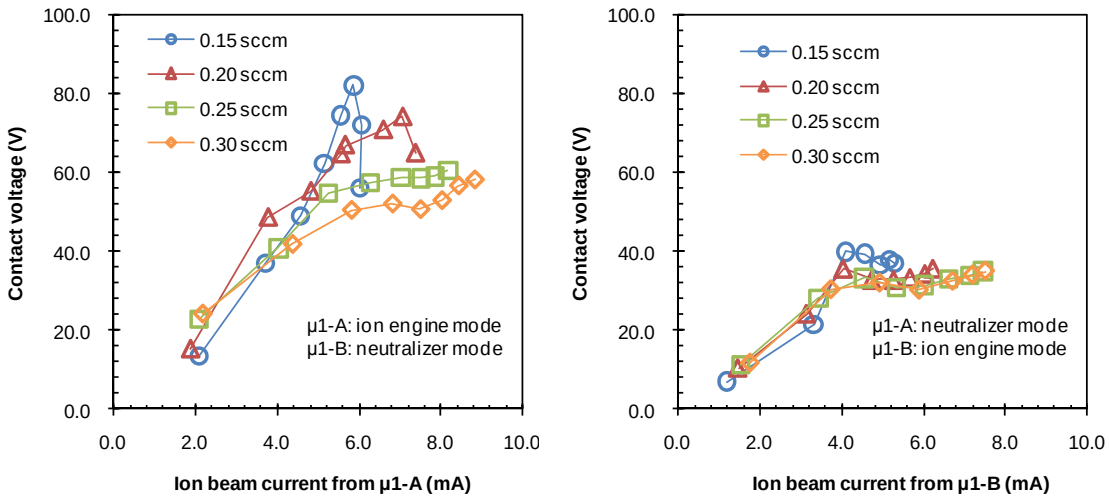

Fig. 13 Contact voltage dependence on the ion beam current using two μ1 thrusters: μ1-A and μ1-B.

IV. Conclusion

The objective of this study was to realize a switching operation of ion engine mode and neutralizer mode using miniature ion engines with sufficient performance for microspacecraft. First, the typical operation of the miniature ion engine μ1 was shown. The μ1 ion engine provide 250 W/A ion production cost and 37% propellant utilization efficiency with the input microwave power of 1.0 W and xenon mass flow rate of 0.15 sccm. Secondly, we measured the fundamental characteristics of electron emission from this ion engine. This was performed by installing a single-aperture orifice plate with the μ1 instead of the grid system and by applying the positive voltage to the collector plate placed outside. This experiment gave us important conclusions: 1) there was a minimum threshold for diameter and 2) the best position was above the ring-antenna. Based on this result, a new grid system dedicated for the switching operation was designed. This grid system has two different types of apertures for ions and electrons respectively. The grid system had sufficient performances to extract ion beam for thrust and to emit electrons for the neutralization. Finally successful demonstration of the switching operation was shown by using two μ1 ion engines. The plasma source consumes 1.0 W microwave power and 0.15 sccm mass flow rate under the typical condition. The thruster can provide 3.3 mA ion beam in ion engine mode and neutralize the same amount of ion beam by the contact voltage below 40 V in neutralizer mode.

Acknowledgments

The present work was supported by a Grant-in-Aid for Exploratory Research, No.19656229, sponsored by the Ministry of Education, Culture, Sports, Science and Technology, Japan.

References

[1] Underwood, C.I., Richardson, G., and Savignol, J., "In-orbit results from the SNAP-1 nanosatellite and its future potential," *Philosophical Transactions of the Royal Society London, Series A*, Vol. 361, No.1802, 2003, pp.199-203.

[2] Funase, R., Nakamura, Y., Nagai, M., Enokuchi, A., Komatsu, M., Nakasuka, S., and Kawakita, S., "Development of COTS-based Pico-Satellite Bus and Its Application to Quick and Low Cost On-orbit Demonstration of Novel Space Technology," *Transactions of the Japan Society for Aeronautical and Space Sciences, Space Technology Japan*, Vol. 6, 2008, pp.1-9.

[3] Saito, H., "An Overview and Initial In-Orbit Status of "INDEX" Satellite," *The 25th International Symposium on Space Technology and Science*, 2006, ISTS 2006-keynote-04v.

[4] Kitts, C., Ronzano, K., Rasay, R. Mas, I., Williams, P., Mahacek, P., Minelli, G., Hines, J., Agasid, E., Friedericks, C., Piccini, M., Parra, M., Timucin, L., Beasley, C., Henschke, M., Luzzi, E., Mai, N., McIntyre, M., Ricks, R., Squires, D., Storment, C., Tucker, J., Yost, B., Defouw, G., and Ricco, A., "Flight Results from the GeneSat-1 Biological Microsatellite Mission," *Proceedings of the 21nd Annual Small Satellite Conference*, 2007.

[5] O'Donnell Jr., J.R., Concha, M., Tsai, D.C., Placanica, S.J., Morrissey, J.R., Russo, A.M., "Space technology 5 launch and operations," *Advances in the Astronautical Sciences*, Vol. 128, 2007, p 735-753.

[6] Fong, C.J., Shiau, W.T., Lin, C.T., Kuo, T.C., Chu, C.H., Yang, S.K., Yen, N.L., Chen, S.S., Kuo, Y.H., Liou, Y.A., and Chi, S., "Constellation deployment for the FORMOSAT-3/COSMIC mission," *IEEE Transactions on Geoscience and Remote Sensing*, Vol. 46, No. 11, 2008, pp.3367-79.

[7] Nakamura, Y. and Hashimoto, H., "SOHLA-1 - Low cost satellite development with technology transfer program of JAXA," *56th International Astronautical Congress*, Vol.4, 2005, pp.2413-2418.

[8] Komatsu, M., "University of Tokyo Nano Satellite Project "PRISM"," *The 26th International Symposium on Space Technology and Science*, 2008, ISTS 2008-s-08.

[9] Micci, M. M., and Ketsdever, A. D., Micropropulsion for Small Spacecraft, American Institute of Aeronautics and Astronautics, Washington, D.C., 2000.

[10] Goebel, D.M. and Katz, I., Fundamentals of Electric Propulsion, Wiley, New Jersey, 2008.

[11] Wirz, R.E., "Discharge Plasma Process of Ring-Cusp Ion Thrusters," Ph.D. Dissertation, California Inst. of Technology, Pasadena, 2005.

[12] Wirz, R.E., Gale, M., Mueller, J., and Marrese, C., "Miniature Ion Thrusters for Precision Formation Flying", AIAA paper 2004-4115.

[13] Felli, D., Loeb, H.W., Schartner, K.H., Weis, S., Krimse, D., Meyer, B.K., Killinger, R., Muller, H., and Di Cara, D.M., "Performance Mapping of New μN-RITs at Giessen," IEPC Paper 2005-265.

[14] Takao, Y., Masui, H., Miyamoto, T., Kataharada, H., Ijiri, H., Nakashima, H., "Development of Small-Scale Microwave Discharge Ion Thruster," *Vacuum*, Vol. 73, 2003, 449 – 454.

[15] Yamamoto, N., Masui, H., Kataharada, H., Nakashima, H., and Takao, Y., "Antenna Configuration Effects on Thrust Performance of Miniature Microwave Discharge Ion Engine," *Journal of Propulsion and Power*, Vol. 22, No. 4, 2006, pp.925 – 928.

[16] Nakayama, Y., Funaki, I., and Kuninaka, H., "Sub-Milli-Newton Class Miniature Microwave Ion Thruster," *Journal of Propulsion and Power*, Vol. 23, No. 2, 2007, pp. 495-499.

[17] Yamamoto, N., Kondo, S., Chikaoka, T., Nakashima, H., and Takao, Y., "Effects of magnetic field configuration on thrust performance in a miniature microwave discharge ion engine," *Journal of Applied Physics*, Vol. 102, No. 123304, 2007.

[18] Koizumi, H. and Kuninaka, H., "Antenna Design Method for Low Power Miniaturized Microwave Discharge Ion Engines," *J. JSASS*, **57** (2009).

[19] Kuninaka, H. and Satori, S., "Development and Demonstration of a Cathode-less Electron Cyclotron Resonance Ion Thruster," *Journal of Propulsion and Power*, Vol. 14, No. 6, 1998, pp.1022-1026.

[20] Kuninaka, H., Nishiyama, K., Shimizu, Y., Toki, K., and Kawaguchi, J., "Initial Operation of Microwave Discharge Ion Engines Onboard 'HAYABUSA' Asteroid Explorer," *Journal of the Japan Society for Aeronautical and Space Science*, Vol. 52, No. 602, 2004, pp.129-134.(Japanese)

[21] Kuninaka, H., Nishiyama, K., Funaki, I., Yamada, T., Shimizu, Y., and Kawaguchi, J., "Powered Flight of Electron Cyclotron Resonance Ion Engines on Hayabusa Explorer," *Journal of Propulsion and Power*, Vol. 23, No. 3, 2007, pp.544-551.

[22] Koizumi, H., and Kuninaka, H., "Proposal and Fundamental Experiment of the Distributed Miniature Ion Engine System μ1," Proceedings of Space Transportation Symposium FY2007, 2008, pp.395-398. (Japanese).

[23] Koizumi, H., and Kuninaka, H., "Low Power Micro Ion Engine Using Microwave Discharge," Joint Propulsion Conference, AIAA Paper 2008-4531.